

The Intrinsic Temperature and Radiative-Convective Boundary Depth in the Atmospheres of Hot Jupiters

DANIEL THORNGREN,¹ PETER GAO,² AND JONATHAN J. FORTNEY³

¹*Department of Physics, University of California, Santa Cruz*

²*51 Pegasi b Fellow, Department of Astronomy, University of California, Berkeley*

³*Department of Astronomy and Astrophysics, University of California, Santa Cruz*

ABSTRACT

In giant planet atmosphere modelling, the intrinsic temperature T_{int} and radiative-convective boundary (RCB) are important lower boundary conditions. Often in one-dimensional radiative-convective models and in three-dimensional general circulation models it is assumed that T_{int} is similar to that of Jupiter itself, around 100 K, which yields a RCB around 1 kbar for hot Jupiters. In this work, we show that the inflated radii, and hence high specific entropy interiors, of hot Jupiters suggest much higher T_{int} values. Assuming the effect is primarily due to current heating (rather than delayed cooling), we derive an equilibrium relation between T_{eq} and T_{int} , showing that the latter can take values as high as 700 K. In response, the RCB moves upward in the atmosphere. Using one-dimensional radiative-convective atmosphere models, we find RCBs of only a few bars, rather than the kilobar typically supposed. This much shallower RCB has important implications for the atmospheric structure, vertical and horizontal circulation, interpretations of phase curves, and the effect of deep cold traps on cloud formation.

Keywords: planets and satellites: atmospheres – planets and satellites: gaseous planets – planets and satellites: interiors – planets and satellites: physical evolution

1. INTRODUCTION

Soon after the discovery of strongly irradiated giant planets (Mayor & Queloz 1995), it was realized that they would have strikingly different atmospheres from the giant planets in our own solar system (Guillot et al. 1996; Seager & Sasselov 1998; Marley et al. 1999). For Jupiter at optical wavelengths, one can see down to the ammonia cloud tops (~ 0.6 bars), which are within the convective region of the planet that extends into its vast deep interior. For hot Jupiter atmospheres, it was appreciated that they could remain radiative to a considerably greater depth due to high incident fluxes that forces the upper atmosphere to a much higher temperature than for an isolated object. (Guillot & Showman 2002; Showman & Guillot 2002; Sudarsky et al. 2003). This leads to a significant departure of the atmospheric temperature structure from an adiabat, and has major consequences for atmospheric circulation (Showman & Guillot 2002; Showman et al. 2008; Rauscher & Menou 2013; Heng & Showman 2015). As such, there has long been significant interest in understanding what controls the pressure level of the hot Jupiter radiative-convective boundary (RCB).

Radiative-convective atmosphere models for hot Jupiters found that, for Jupiter-like intrinsic fluxes (pa-

rameterized by T_{int} , of 100 K) but incident stellar fluxes 10^4 times larger, one typically found RCB pressures near 1 kbar (e.g., Guillot & Showman 2002; Sudarsky et al. 2003; Fortney et al. 2005). While it was understood early on that the RCB depth strongly depends on the value of T_{int} (e.g. Sudarsky et al. 2003, their Figure 16), cooling models suggested that T_{int} values would fall with time to Jupiter-like values (Guillot & Showman 2002; Burrows et al. 2004; Fortney et al. 2007), and the ~ 1 kbar RCB became ensconced as a “typical” value for these objects. Such atmospheres are very different from those found in the solar system, so considerable modeling effort has gone into studying their possible vertical and horizontal circulation patterns, and to what degree cold traps at depth may affect what molecules and cloud species can be seen in the visible layers (Hubeny et al. 2003; Fortney et al. 2008; Powell et al. 2018).

However, the larger than expected radii of hot Jupiters suggest interiors that are much hotter and more luminous than our own Jupiter. This should directly lead to higher interior fluxes and shallower – sometimes much shallower – RCB boundaries than the canonical 1 kbar. Such atmospheres have occasionally appeared in other works (Guillot 2010; Sing et al. 2016; Tremblin et al. 2017; Komacek & Youdin 2017, e.g.), but not studied ex-

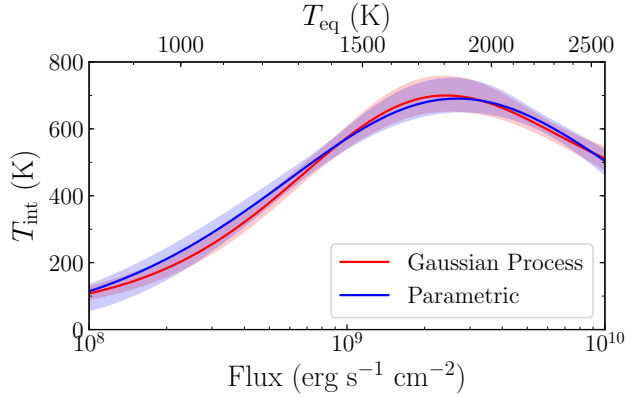


Figure 1. The intrinsic temperatures of hot Jupiters in equilibrium as a function of incident flux (bottom) or equilibrium temperature (top). These were derived from the two favored heating models (Gaussian process and Gaussian parametric) of [Thorngren & Fortney \(2019\)](#), using Eq. 2, with corresponding uncertainties. The two models yield nearly identical results. Importantly, the intrinsic temperatures must be quite high – up to 700K – to match the hot interiors required to explain their radii.

tensively. In this work, we will quantify interior fluxes and the RCB depth as a function of planetary T_{eq} to better inform the thermal structure of 1D and 3D atmosphere models.

2. MODELLING

We will parameterize the rate at which heat escapes from a planet’s deep interior using the intrinsic temperature T_{int} . Its value is primarily driven by the entropy of the underlying adiabat. Thus, high T_{int} is typical of young exoplanets and inflated hot Jupiters. If the mechanism inflating hot Jupiters involves the deposition of heat into the interior, then they will eventually reach a thermal equilibrium where $E_{\text{in}} = E_{\text{out}}$. The hotter the planet, the faster this equilibrium will be reached, in as little as tens of megayears ([Thorngren & Fortney 2018](#)). Once equilibrium is reached, the intrinsic temperature is a function of the equilibrium temperature:

$$4\pi R^2 \sigma T_{\text{int}}^4 = \pi R^2 F \epsilon(F) \quad (1)$$

$$T_{\text{int}} = \left(\frac{F \epsilon(F)}{4\sigma} \right)^{\frac{1}{4}} = \epsilon(F)^{\frac{1}{4}} T_{\text{eq}} \quad (2)$$

$$\approx 1.24 T_{\text{eq}} \exp \left(-\frac{(\log(F) - .14)^2}{2.96} \right) \quad (3)$$

Here, F is the incident flux on the planet (so $F = 4\sigma T_{\text{eq}}^4$), σ is the Stefan-Boltzmann constant, and ϵ is the fraction of the flux which heats the interior. This varies with flux, and was inferred by matching model planets with the observed hot Jupiter population in ([Thorngren](#)

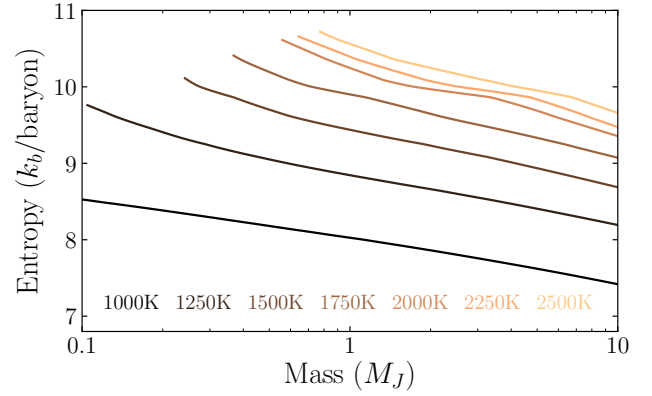


Figure 2. The equilibrium entropy of hot Jupiters as a function of their mass for various equilibrium temperatures. Each line has models of the same intrinsic and equilibrium temperature, but variations in the resulting surface gravity lead to different internal entropies. In particular, heat escapes more efficiently through the compact atmospheres of massive objects for a given T_{int} . The composition was assumed to be typical (from [Thorngren et al. 2016](#)), using the SCvH ([Saumon et al. 1995](#)) and ANEOS 50-50 rock-ice ([Thompson 1990](#)) equations of state; different compositions will shift the entropy somewhat.

& Fortney 2018). The resulting intrinsic temperatures are shown in Figure 1, and the associated entropy (which depend on mass and composition), are shown in Figure 2.

The high intrinsic temperatures this relation produces are important due to the effect they have on the atmosphere. In particular, the radiative-convective boundary moves to lower pressures for higher T_{int} . In contrast, larger T_{eq} tends to push the RCB to higher pressures. As these temperatures are related, it is not immediately obvious where the RCB ends up for planets at high equilibrium temperatures. To evaluate the RCB depth, we generate model atmospheres using a well-established thermal structure model for exoplanets and brown dwarfs (e.g. [McKay et al. 1989](#); [Marley et al. 1996, 1999](#); [Fortney et al. 2005, 2008](#); [Saumon & Marley 2008](#); [Morley et al. 2012](#)). The model computes temperature–pressure (TP) and composition profiles assuming radiative–convective–thermochemical equilibrium, taking into account depletion of molecular species due to condensation.

Model atmospheres are generated for a grid of cloud-free giant exoplanets with 1 bar gravities of 4, 10, and 25 m s^{-2} and a range of T_{eq} from ~ 700 to ~ 2800 K, computed assuming full heat redistribution (Figure 3). Functionally, we positioned the model planets at various semi-major axes around a sun-like star. Two grids were computed, one assuming solar atmospheric metal-

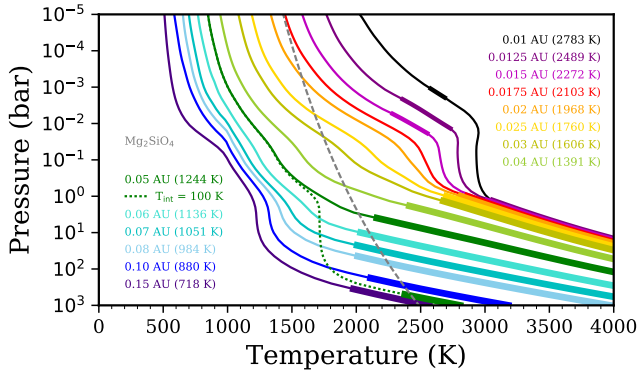


Figure 3. The pressure-temperature profiles of our $10\times$ solar atmospheric metallicity models for various semi-major axes around a sun-like star and the resulting T_{eq} (in brackets), from which we derive the intrinsic temperature. The thick lines indicate convective regions, whereas thin lines correspond to radiative regions. An alternative pressure-temperature profile for a $T_{\text{int}} = 100$ K model for the 0.05 AU case is plotted in the dotted curve. The condensation curve for forsterite, Mg_2SiO_4 , is shown in the gray dashed curve. In the hottest cases, a second convective region forms; however, we will use the term RCB to refer exclusively to the outer edge of the interior adiabetic envelope. This boundary is visible in the plot for the profiles given, and moves to lower pressures at higher equilibrium temperatures.

licity and one assuming $10 \times$ solar atmospheric metallicity, with any additional heavy elements sequestered in a core, such that the bulk metallicities matched the median of the observed mass-metallicity relationship given by Thorngren et al. (2016). The RCB depth for each model planet is then defined as the highest pressure level where the local lapse rate transitions from adiabatic to subadiabatic.

We calculate the masses, radii, and adiabat entropies (Figure 2) of our model planets (from the gravity and T_{eq}) using the planetary interior model of Thorngren & Fortney (2018), which solves the equations of hydrostatic equilibrium, mass and energy conservation, and an appropriately chosen equation of state. We use the SCvH (Saumon et al. 1995) EOS for a solar ratio mixture of hydrogen and helium, and the ANEOS 50-50 rock-ice EOS (Thompson 1990) for the metals.

It is important to consider the effect that our assumptions about the hot Jupiter heating have on the model. In Thorngren & Fortney (2018), it was assumed that the heating was proportional to and a function of the incident flux, based on the results of Weiss et al. (2013). There may be additional factors that affect the heating, such as planet and stellar mass, but since $\epsilon(F)$ seems to predict planetary radii quite well, these likely add at most modest uncertainty to our estimates of T_{int} . An additional consideration is whether the anomalous radii

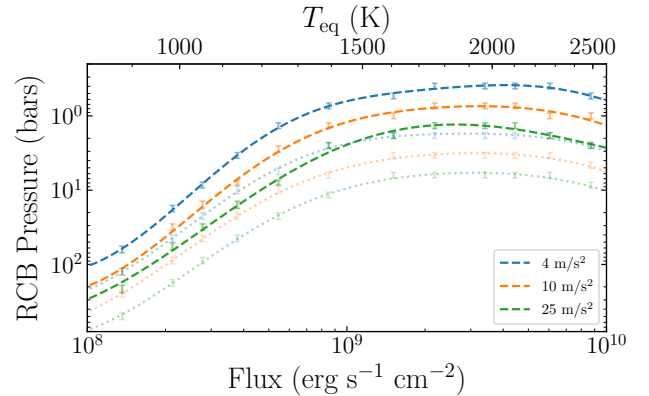


Figure 4. The RCB pressure as a function of incident flux (or T_{eq}), shown for different surface gravities (colors, see legend) and $1\times$ (pale dotted) and $10\times$ (dashed) solar metallicity atmospheres. Due to binning effects, there are small uncertainties around the modeled points, so we drew smooth lines through the data using Gaussian process interpolation with a squared exponential kernel whose parameters were optimized via the maximum likelihood.

are caused entirely by heating, or whether there is a delayed cooling effect as well; for example, Ohmic dissipation (Batygin et al. 2011) may be a combination of these (Wu & Lithwick 2013; Ginzburg & Sari 2016). Delayed cooling effects would alter the apparent T_{int} for a given internal adiabat entropy, and delay arrival at thermal equilibrium. However, many anomalous heating models do not rely on delayed cooling (e.g. Arras & Socrates 2009; Youdin & Mitchell 2010; Tremblin et al. 2017), and signs of possible reinflation (Hartman et al. 2016; Grunblatt et al. 2016, 2017) seem to favor these. If reinflation is conclusively shown to occur, then anomalous heating must be the dominant cause of radius inflation (Lopez & Fortney 2016), and our T_{int} estimates will be particularly good. Finally, the usual uncertainties in the equation of state (see e.g. Militzer & Hubbard 2013; Chabrier et al. 2019) and planet interior structure (Baraffe et al. 2008; Leconte & Chabrier 2012) discussed in Thorngren et al. (2016) also apply to this work.

3. RESULTS AND DISCUSSION

Our results for the location of the RCB are shown in Figure 4. The RCB moves to lower pressures at higher equilibrium temperatures, roughly in line with how T_{int} varies with T_{eq} . At the inflation cutoff of around 1000 K (Miller & Fortney 2011), the RCB is found at around 100 bars. At the extremum around $T_{\text{eq}} = 1800$ K, it is found at roughly 1 bar. Higher gravity moves the RCB to higher pressures, and higher metallicity moves it to lower pressures. At equilibrium, no hot Jupiter with

gravity $< 25 \text{ m s}^{-2}$ and solar or supersolar atmospheric metallicity should have an RCB as deep as 1 kbar.

These results have important implications for understanding the anomalous heating of hot Jupiters. Heating deposited below the RCB is much more effective for inflating planets than heat deposited above (Komacek & Youdin 2017; Batygin & Stevenson 2010). This is particularly important for Ohmic dissipation. For a lower RCB pressure, models like Ohmic dissipation will be more efficient than previously considered. Since giant planets are born quite hot, they will have RCBs at low pressures at young ages that could be maintained there by this heating. However, this would not necessarily allow for reinflation of a planet whose interior has already cooled (see Lopez & Fortney 2016), as the RCB might already be at high pressures when the heating started. We refer the reader to Komacek & Youdin (2017) for a more detailed and broader discussion of these heating deposition depth effects.

Perhaps the most important implications are those for the global circulation models (GCMs) of hot Jupiters. It has long been a convention in this field to use intrinsic temperatures similar to Jupiter’s (e.g. Showman et al. 2015; Amundsen et al. 2016; Komacek et al. 2017; Lothringer et al. 2018; Flowers et al. 2019, and many others), around 100 K (Li et al. 2012). Our work shows that more realistic values for T_{int} should depend strongly on the incident flux and will typically be several hundreds of Kelvin, as shown in Figure 1. Furthermore, this difference is important for vertical mixing and circumplanetary circulation, as it shifts the RCB to considerably lower pressures. It was recently demonstrated in the hot Jupiter context that changing the lower boundary conditions can yield significantly different atmospheric flows in these simulations (see Carone et al. 2019).

The higher implied intrinsic fluxes could also impact interpretations of the observed flux from hot Jupiters. For phase curves, night-side fluxes will be a mix of intrinsic flux, which in many cases can no longer be thought of as negligible, in addition to energy transported from the day side. Even on the day side, in near-infrared opacity windows that probe deeply, one might be able to observe this intrinsic flux as a small perturbation on the day-side emission spectrum (e.g., Fortney et al. 2017).

The value of T_{int} is also important for the location and abundance of condensates in hot Jupiter atmospheres. Figure 3 compares the condensation curve of forsterite to our model TP profiles; the intersection between the condensation curve and the TP profile delineates the forsterite cloud base. Previous works that considered low T_{int} atmospheres have hypothesized the existence of deep “cold traps” for hot Jupiter clouds, where a cloud base at high pressures (> 100 bars) removes condensates and condensate vapor from the visible layers of the atmosphere (e.g. Spiegel et al. 2009; Parmentier et al. 2016). However, higher T_{int} values increase deep atmospheric temperatures, such that the cloud base is much shallower in the atmosphere. For example, at $T_{\text{eq}} = 1244$ K, whether $T_{\text{int}} = 100$ K or the nominal value computed in this work can result in differences in the forsterite cloud base pressure of ~ 2 dex (Figure 3). This can have important observable consequences, particular in emission, where the lack of deep cold traps could result in cloudier dayside atmospheres (Powell et al. 2018).

Future work should focus on the effects that these altered boundary conditions have on the cloud structure, spectra, and day-night contrasts of hot Jupiters. As we learn more about hot Jupiter interiors through theoretical development, population studies (especially from new TESS discoveries) and potentially reinflated giants (Grunblatt et al. 2017), we can better characterize these important atmospheric boundary conditions.

REFERENCES

- Amundsen, D. S., Mayne, N. J., Baraffe, I., et al. 2016, *A&A*, 595, A36
- Arras, P., & Socrates, A. 2009, ArXiv e-prints, 0901, arXiv:0901.0735
- Baraffe, I., Chabrier, G., & Barman, T. 2008, *Astronomy and Astrophysics*, 482, 315
- Batygin, K., & Stevenson, D. J. 2010, *ApJL*, 714, L238
- Batygin, K., Stevenson, D. J., & Bodenheimer, P. H. 2011, *The Astrophysical Journal*, 738, 1
- Burrows, A., Hubeny, I., Hubbard, W. B., Sudarsky, D., & Fortney, J. J. 2004, *The Astrophysical Journal*, 610, L53
- Carone, L., Baeyens, R., Mollière, P., et al. 2019, arXiv e-prints, arXiv:1904.13334
- Chabrier, G., Mazevet, S., & Soubiran, F. 2019, *The Astrophysical Journal*, 872, 51
- Flowers, E., Brogi, M., Rauscher, E., Kempton, E. M.-R., & Chiavassa, A. 2019, *The Astronomical Journal*, 157, 209
- Fortney, J. J., Marley, M. S., & Barnes, J. W. 2007, *The Astrophysical Journal*, 659, 1661
- Fortney, J. J., Marley, M. S., Lodders, K., Saumon, D., & Freedman, R. 2005, *ApJ*, 627, L69
- Fortney, J. J., Marley, M. S., Saumon, D., & Lodders, K. 2008, *The Astrophysical Journal*, 683, 1104

- Fortney, J. J., Thorngren, D., Line, M. R., & Morley, C. 2017, AAS/Division for Planetary Sciences Meeting Abstracts #49, 408.04
- Ginzburg, S., & Sari, R. 2016, *The Astrophysical Journal*, 819, 116
- Grunblatt, S. K., Huber, D., Gaidos, E. J., et al. 2016, *The Astronomical Journal*, 152, 185
- Grunblatt, S. K., Huber, D., Gaidos, E., et al. 2017, *The Astronomical Journal*, 154, 254
- Guillot, T. 2010, *Astronomy and Astrophysics*, 520, A27
- Guillot, T., Burrows, A., Hubbard, W. B., Lunine, J. I., & Saumon, D. 1996, *The Astrophysical Journal*, 459, L35
- Guillot, T., & Showman, A. P. 2002, *Astronomy and Astrophysics*, 385, 156
- Hartman, J. D., Bakos, G. Á., Bhatti, W., et al. 2016, *The Astronomical Journal*, 152, 182
- Heng, K., & Showman, A. P. 2015, *Annual Review of Earth and Planetary Sciences*, 43, 509
- Hubeny, I., Burrows, A., & Sudarsky, D. 2003, *The Astrophysical Journal*, 594, 1011
- Komacek, T. D., Showman, A. P., & Tan, X. 2017, *The Astrophysical Journal*, 835, 198
- Komacek, T. D., & Youdin, A. N. 2017, *The Astrophysical Journal*, 844, 94
- Leconte, J., & Chabrier, G. 2012, *A&A*, 540, A20
- Li, L., Baines, K. H., Smith, M. A., et al. 2012, *Journal of Geophysical Research: Planets*, 117, n/a
- Lopez, E. D., & Fortney, J. J. 2016, *The Astrophysical Journal*, 818, 4
- Lothringer, J. D., Barman, T., & Koskinen, T. 2018, *The Astrophysical Journal*, 866, 27
- Marley, M. S., Gelino, C., Stephens, D., Lunine, J. I., & Freedman, R. 1999, *The Astrophysical Journal*, 513, 879
- Marley, M. S., Saumon, D., Guillot, T., et al. 1996, *Science*, 272, 1919
- Mayor, M., & Queloz, D. 1995, *Nature*, 378, 355
- McKay, C. P., Pollack, J. B., & Courtin, R. 1989, *Icarus*, 80, 23
- Militzer, B., & Hubbard, W. B. 2013, *The Astrophysical Journal*, 774, 148
- Miller, N., & Fortney, J. J. 2011, *The Astrophysical Journal Letters*, 736, L29
- Morley, C. V., Fortney, J. J., Marley, M. S., et al. 2012, *The Astrophysical Journal*, 756, 172
- Parmentier, V., Fortney, J. J., Showman, A. P., Morley, C., & Marley, M. S. 2016, *The Astrophysical Journal*, 828, 22
- Powell, D., Zhang, X., Gao, P., & Parmentier, V. 2018, *The Astrophysical Journal*, 860, 18
- Rauscher, E., & Menou, K. 2013, *The Astrophysical Journal*, 764, 103
- Saumon, D., Chabrier, G., & van Horn, H. M. 1995, *The Astrophysical Journal Supplement Series*, 99, 713
- Saumon, D., & Marley, M. S. 2008, *The Astrophysical Journal*, 689, 1327
- Seager, S., & Sasselov, D. D. 1998, *The Astrophysical Journal*, 502, L157
- Showman, A. P., & Guillot, T. 2002, *Astronomy and Astrophysics*, 385, 166
- Showman, A. P., Lewis, N. K., & Fortney, J. J. 2015, *The Astrophysical Journal*, 801, 95
- Showman, A. P., Menou, K., & Cho, J. Y.-K. 2008, *Extreme Solar Systems*, 398, 419
- Sing, D. K., Fortney, J. J., Nikolov, N., et al. 2016, *Nature*, 529, 59
- Spiegel, D. S., Silverio, K., & Burrows, A. 2009, *The Astrophysical Journal*, 699, 1487
- Sudarsky, D., Burrows, A., & Hubeny, I. 2003, *The Astrophysical Journal*, 588, 1121
- Thompson, S. L. 1990, ANEOS Analytic Equations of State for Shock Physics Codes Input Manual, Tech. Rep. SAND-89-2951, 6939284, Sandia National Laboratory, doi:10.2172/6939284
- Thorngren, D., & Fortney, J. J. 2019, *The Astrophysical Journal*, 874, L31
- Thorngren, D. P., & Fortney, J. J. 2018, *The Astronomical Journal*, 155, 214
- Thorngren, D. P., Fortney, J. J., Murray-Clay, R. A., & Lopez, E. D. 2016, *The Astrophysical Journal*, 831, 64
- Tremblin, P., Chabrier, G., Mayne, N. J., et al. 2017, *The Astrophysical Journal*, 841, 30
- Weiss, L. M., Marcy, G. W., Rowe, J. F., et al. 2013, *The Astrophysical Journal*, 768, 14
- Wu, Y., & Lithwick, Y. 2013, *The Astrophysical Journal*, 763, 13
- Youdin, A. N., & Mitchell, J. L. 2010, *The Astrophysical Journal*, 721, 1113